High Affinity Interaction between a Synthetic, Highly Negatively Charged Pentasaccharide and α- or β-Antithrombin Is Predominantly Due to Nonionic Interactions†

Rebecka Hjelm and Sophia Schedin-Weiss*

Department of Medical Biochemistry and Microbiology, Uppsala University, Uppsala Biomedical Center, Box 582, SE-751 23 Uppsala, Sweden

Received December 4, 2006; Revised Manuscript Received January 19, 2007

ABSTRACT: Idraparinux is a synthetic O-sulfated, O-methylated pentasaccharide that binds tightly to antithrombin (AT) and thereby specifically and efficiently induces the inactivation of the procoagulant protease, factor Xa. In this study, the affinity and kinetics of the interaction of this high-affinity pentasaccharide with α- and β-AT were compared with those of a synthetic pentasaccharide comprising the natural AT-binding sequence of heparin. Dissociation equilibrium constants, K_d, for the interactions of Idraparinux with α- and β-AT were approximately 0.4 and 0.1 nM, respectively, corresponding to an over 100-fold enhancement in affinity compared with that of the normal pentasaccharide. This large enhancement was due to a ∼400-fold tighter conformationally activated complex formed in the second binding step, whereas the encounter complex established in the first step was ∼4-fold weaker. The high-affinity and normal pentasaccharides both made a total of four ionic interactions with AT, although the high-affinity saccharide only established one ionic interaction in the first binding step and was compensated by three in the second step, whereas the normal pentasaccharide established two ionic interactions in each step. In contrast, the affinities of the nonionic interactions (K_d ∼450 and 90 nM for the binding to α- and β-AT, respectively) were considerably higher than those for the normal pentasaccharide and the highest of all AT−saccharide interactions reported so far. The nonionic contribution to the total free energy of the high-affinity pentasaccharide binding to AT thus amounted to ∼70%. These findings show that nonionic interactions can play a predominant role in the binding of highly charged saccharide ligands to proteins and can be successfully exploited in the design of such biologically active ligands.

Antithrombin (AT)[1] is the most potent physiological anticoagulant protease inhibitor in blood through its ability to efficiently inhibit procoagulant proteases, mainly factor IXa, factor Xa, and thrombin (*1*). It is a serine protease inhibitor belonging to the serpin superfamily of proteins and is classified as serpin C1 (*2*). AT inhibits its target proteases by a suicide mechanism, involving a substantial conformational change of the inhibitor that leads to trapping of the inactivated protease in a 1:1 complex in the acyl-enzyme state with a half-life of 0.5−3 days (*3*, *4*). The inhibitory activity of AT can be enhanced up to 10^5-fold by heparin/heparan sulfate or synthetic analogues, resulting in inhibition rate constants of 10^6-10^7 M^{-1} s^{-1} (*1*). The enhanced inhibitory activity is partially due to a conformational change induced by binding of a specific pentasaccharide sequence found in heparin (*5*) that allosterically activates the inhibitor and partially due to a bridging mechanism that brings the protease and inhibitor into a ternary complex. The bridging mechanism plays a predominant role in the heparin-induced inactivation of thrombin by AT, whereas the conformational change is of major importance for the corresponding inactivation of factor Xa (*1*).

The accelerating effects of heparin or synthetic analogues on the rates of AT−protease reactions make these saccharides highly useful as anticoagulant drugs. Pentasaccharides that induce the allosteric activation of AT are attractive in this respect because they are more specific than longer heparin chains and selectively enhance the inhibitory activity of AT toward factor Xa (*6*). The pentasaccharide binding site of AT has been elucidated from mutagenesis studies and crystal structures (*7*−*17*).

Not only the protein structure itself but also the *N*-glycans attached to AT affect the affinity of heparin or pentasaccharides for the protein. Two N-glycosylation variants of AT exist in human blood plasma: α-AT, which is N-glycosylated at all four potential N-glycosylation sites, and β-AT, which lacks one of the four *N*-glycans at Asn 135 (*18*). Heparin and pentasaccharides bind with higher affinity to the β-variant because of the *N*-glycan at Asn 135 sterically hindering the conformational change step of the interaction.

† This work was supported by Swedish Research Council Grants 2003-6107 and 2005-6412 (to S.S.W.) and by the Linnéus Foundation for Medical Research (S.S.W.).

* To whom correspondence should be addressed. Phone: +46-18-4716655. Fax: +46-18-4714673. E-mail: Sophia.Schedin_Weiss@imbim.uu.se.

[1] Abbreviations: AT, antithrombin; PAGE, polyacrylamide gel electrophoresis; SDS, sodium dodecyl sulphate; K_d, dissociation equilibrium constant; k_{obs}, observed pseudo-first order rate constant; k_{on}, bimolecular association rate constant; k_{off}, dissociation rate constant; K_1, dissociation equilibrium constant of the first binding step; k_{+2}, forward rate constant of the second binding step; k_{-2}, reverse rate constant of the second binding step.

10.1021/bi6024929 CCC: $37.00
Published on Web 02/27/2007

After the discovery of the pentasaccharide sequence of heparin that binds with high affinity to AT (*5*), methods to produce this pentasaccharide by organic synthesis were developed. The α-methyl-glycoside form of the natural pentasaccharide sequence was synthesized first (*19*). Today, it is in clinical use as Fondaparinux (*20*). Attempts to develop more easily manufactured compounds with improved pharmacological properties led to a more extensively modified high-affinity pentasaccharide, Idraparinux (*21*). The latter has a prolonged plasma half-life compared with that of the natural pentasaccharide and is now in a late stage of clinical development.

Although the different heparins and synthetic analogues that are clinically used are continuously improving, there are still limitations to their usefulness. The ultimate goal is to design small, specific compounds that are easily manufactured and that can be orally administered. In this study, we have characterized the interaction between the high-affinity pentasaccharide, Idraparinux, and human α- and β-AT. Our work revealed that a surprisingly large nonionic contribution (with nonionic K_d values in the nanomolar range) accounted for most of the affinity of the highly negatively charged pentasaccharide for both AT variants. Nonionic interactions can thus be of major importance in the binding of highly ionic saccharide ligands to proteins.

EXPERIMENTAL PROCEDURES

Proteins and Pentasaccharides. The α- and β-variants of AT were purified from fresh frozen human blood plasma from healthy donors by heparin-Sepharose chromatography, followed by DEAE-Sephadex ion-exchange chromatography and Sephacryl S-200 gel chromatography (*18*, *22*). All chromatographic media were purchased from GE Healthcare Bio-Sciences, Uppsala, Sweden. The purity of the AT fractions was analyzed by native PAGE and SDS−PAGE under reducing conditions. Protein concentrations were determined from the absorbance at 280 nm with the use of a molar extinction coefficient of 37 700 M^{-1} cm^{-1} (*23*). α-AT purified by this procedure is 100% active (*22*). This was verified by titrations with full-length high-affinity heparin of known concentration, which was donated by Professor Steven Olson, University of Illinois, Chicago (*22*, *24*). The active concentration of β-AT was determined from the stoichiometry of thrombin inhibition (*18*) and heparin binding.

Bovine thrombin was prepared from prothrombin that was donated by Professor Johan Stenflo, Lund University, Sweden (*25*). The active thrombin concentration was measured by titrations with 100% active α-AT (*22*).

The synthetic high-affinity pentasaccharide, Idraparinux, also denoted as SR34006, was supplied by Sanofi-Aventis. The molar concentration of a stock solution of the pentasaccharide in water was determined by stoichiometric titrations against 100% active α-AT.

Fluorescence Titrations. Equilibrium binding was analyzed by titrating Idraparinux into a fixed concentration of AT while monitoring the increase in tryptophan fluorescence accompanying the interaction (*26*, *27*) in an SLM 4800S spectrofluorimeter (SLM Instruments, Rochester, NY) as described previously (*24*, *28*). Stoichiometric titrations were done at an ionic strength of 0.15 with 1 μM protein, whereas affinity titrations were done at ionic strengths of 0.3 to 0.8 with 100−200 nM protein. Binding stoichiometry and dissociation equilibrium constants were determined by fitting the data to the equilibrium binding equation by nonlinear least-squares analysis (*22*).

Rapid Kinetics. The kinetics of high-affinity pentasaccharide binding to AT was measured by monitoring the fluorescence increase accompanying the interaction in an SX-17MV stopped-flow instrument (Applied Photophysics, Leatherhead, U.K.) as described previously (*10*) at ionic strengths varying between 0.1 and 0.6. Pseudo-first-order conditions were arranged, with the high-affinity pentasaccharide concentration being at least 10-fold higher than the AT concentration, except at the lowest pentasaccharide concentration (0.1 μM) for which a 5-fold excess was used. Observed pseudo-first-order rate constants, k_{obs}, were obtained by fitting the progress curves to a single-exponential function by nonlinear regression. Three to five fluorescence traces were averaged for each k_{obs} determination, the final k_{obs} values reported representing the mean ± SE of 3−5 such determinations.

Experimental Conditions. All equilibrium binding and kinetic studies were performed at 25 ± 0.2 °C in 20 mM sodium phosphate buffer at pH 7.4, containing 100 μM EDTA and 0.1% (w/v) polyethylene glycol 8000. Sodium chloride was added to give the final ionic strengths used in the different experiments.

RESULTS

Homogeneity of the Antithrombin Variants. The preparations of α- and β-AT were >95% homogeneous in native PAGE and SDS−PAGE and fulfilled previously reported migration criteria for the two variants (*18*, *22*). The stoichiometries of heparin binding were 1.0 and 0.90 for the preparations of α- and β-AT, respectively, and the stoichiometry of thrombin inhibition was 0.92 for the β-AT preparation. The concentrations used in equilibrium binding and kinetic experiments were the effective concentrations determined from the stoichiometries of heparin binding.

Affinity of Pentasaccharide Binding. Dissociation equilibrium constants for the binding of the high-affinity pentasaccharide, Idraparinux, to AT were determined by fluorescence titrations. The results were compared with those previously reported for the synthetic pentasaccharide that consists of the heparin sequence that binds with high affinity to AT, presently named Fondaparinux (*18*) (Figure 1), referred to as the normal pentasaccharide in this work. The observed fluorescence enhancement at saturation of AT with the high-affinity pentasaccharide was ∼40%, as previously described for the binding of high-affinity heparin and the normal pentasaccharide to AT (*24*, *26*, *27*). Dissociation constants <∼5 nM could not be determined directly but were obtained from the dependence of K_d on sodium ion concentration described later. Moreover, K_d values >1 μM were calculated from the association and dissociation rate constants (see below). At an ionic strength of 0.15, the K_d values of the high-affinity pentasaccharide binding to α- and β-AT were 0.44 ± 0.14 and 0.13 ± 0.096 nM, respectively, which reflects an affinity at least 100-fold higher than that of the normal pentasaccharide (Table 1). The value for α-AT is comparable with that reported previously (1.4 ± 0.3 nM)

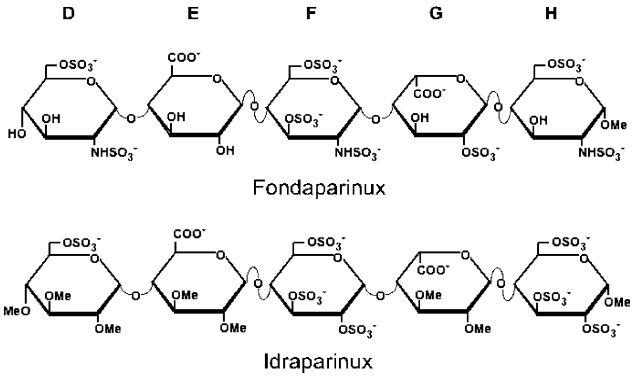

FIGURE 1: Structures of the normal pentasaccharide and Idraparinux. The normal pentasaccharide, Fondaparinux, is a synthetic α-methyl glycoside variant of the pentasaccharide sequence in heparin that binds with high affinity to AT. Idraparinux is an O-sulfated, O-methylated, synthetic analogue designed to improve the pharmacological properties as a potential drug.

(*21*) for the interaction between the high-affinity pentasaccharide and AT (presumably the α-variant), when the experimental errors involved in measuring very low dissociation equilibrium constants by fluorimetry are considered. As previously found for the normal pentasaccharide and high-affinity heparin, the high-affinity pentasaccharide had a higher affinity for *β*-AT than for α-AT (*18*) at all ionic strengths that were compared.

Kinetics of Pentasaccharide Binding. The kinetics of the interactions between Idraparinux and α- and *β*-AT were analyzed by fluorimetry under pseudo-first-order conditions. The fluorescence traces were monophasic and could be satisfactorily fit to a single-exponential function in all experiments. Observed pseudo-first-order rate constants, k_{obs}, were measured at different pentasaccharide concentrations at various ionic strengths. In the low concentration range, 0.1−0.5 *μ*M, the dependence of k_{obs} on the concentration of the high-affinity pentasaccharide was linear at all ionic strengths (inset of Figure 2). The slope of the plots gives the bimolecular association rate constants, k_{on} (Table 1), and the overall dissociation rate constant, k_{off}, can often be determined from the *y*-intercept. For high-affinity pentasaccharide binding to both α- and *β*-AT, however, the k_{off} values were too small to be satisfactorily determined by this method (inset of Figure 2) and were instead calculated from K_d and k_{on} (Table 1). Only at an ionic strength of 0.6 could k_{off} for high-affinity pentasaccharide binding to α-AT be experimentally determined directly with good precision, which gave a value (0.41 ± 0.02 s^{-1}) that is similar to the calculated value. At an ionic strength of 0.15, there was no apparent difference in k_{on} for the high-affinity versus normal pentasaccharide binding to the AT variants, but k_{off} was at least 100-fold lower for the interaction with the high-affinity pentasaccharide. k_{on} for the binding of the high-affinity pentasaccharide to *β*-AT was only 1.4-fold higher than that for the binding to α-AT, whereas k_{off} was approximately 3-fold lower for *β*-AT than for α-AT, which is in agreement with the higher affinity of Idraparinux for *β*-AT than for α-AT.

The dependence of k_{obs} on the concentration of the high-affinity pentasaccharide was extended to higher pentasaccharide concentrations at ionic strengths of 0.1, 0.15, and 0.3 for α-AT and at an ionic strength of 0.15 for *β*-AT. The resulting curves observed for α-AT at all ionic strengths were clearly nonlinear and could be satisfactorily fit to the rectangular hyperbolic equation described in several previous reports on high-affinity heparin and pentasaccharide binding to AT (*18*, *24*, *29*) (Figure 2A). Thus, the behavior is in agreement with the two-step binding mechanism (Scheme 1) established for the binding of high-affinity heparin and the normal pentasaccharide to AT.

Scheme 1

$$AT + H \overset{K_1}{\rightleftharpoons} AT\text{-}H \underset{k_{-2}}{\overset{k_{+2}}{\rightleftharpoons}} AT^*\text{-}H$$

In Scheme 1, H is high-affinity heparin or pentasaccharide, K_1 is the dissociation equilibrium constant for the first, rapid-equilibrium binding step, k_{+2} is the forward rate constant for the second binding step that leads to a conformationally activated state, and k_{-2} is the reverse rate constant for the second binding step. Moreover, $k_{on} = k_{+2}/K_1$ and $k_{off} \approx k_{-2}$ (*24*). The results at an ionic strength of 0.15 reveal that the similarity of the k_{on} values for the interactions of the high-affinity and normal pentasaccharides with α-AT was fortuitous because the two components of k_{on}, that is, K_1 and k_{+2}, were different for the two saccharides. K_1 was thus 4-fold lower and k_{+2} 3-fold higher for the high-affinity pentasaccharide (Table 2). The value of k_{-2} at an ionic strength of 0.15 was >100-fold lower for high-affinity than for normal pentasaccharide binding to α-AT (Table 2). k_{+2}/k_{-2}, which is a measure of the equilibrium position of the second binding step, was 1.9×10^5 for the high-affinity and 500 for the normal pentasaccharide binding to α-AT. The second step of high-affinity pentasaccharide binding is, therefore, ∼400-fold more shifted toward the final, tight complex than that of the normal pentasaccharide. A comparison of K_1 and k_{+2} at ionic strengths of 0.1, 0.15, and 0.3 (Table 2) demonstrated that K_1 was ionic strength-dependent, whereas k_{+2} was not, similar to what has previously been reported for both high-affinity heparin and the normal pentasaccharide (*24*, *29*).

In the case of *β*-AT, the plot of k_{obs} versus high-affinity pentasaccharide concentration at an ionic strength of 0.15 was linear up to the highest k_{obs} that could be measured (because of the dead time of the instrument), preventing the kinetic constants of the two-step mechanism from being determined (Figure 2B). This behavior indicates that the interaction between the high-affinity pentasaccharide and *β*-AT has a higher K_1, a higher k_{+2}, or both compared with that with α-AT. It is reasonable to believe that the difference is in the second step because a previous study showed that the higher affinity of heparin and the normal pentasaccharide for *β*-AT than for α-AT is mainly due to a higher forward rate constant and a lower reverse rate constant of the second binding step (*18*).

Ionic and Nonionic Contributions to Overall Pentasaccharide Binding. The ionic and nonionic contributions to the overall binding of Idraparinux to α- and *β*-AT were determined from the effect of sodium ion concentration on the dissociation equilibrium constants, according to the polyelectrolyte theory (*30*), as described previously for heparin and normal pentasaccharide (*24*, *28*). Double-logarithmic plots of K_d versus sodium ion concentration were linear for both α- and *β*-AT (Figure 3). From these plots, K_d', the dissociation equilibrium constant characterizing the nonionic interactions, and Z, the number of ionic interactions, could be derived from the ordinate intercept and the slope,

Table 1: Dissociation Equilibrium Constants, Bimolecular Association Rate Constants, and Dissociation Rate Constants for the Interactions of Idraparinux and Normal Pentasaccharide with α- and β-AT at 25 °C and pH 7.4

pentasaccharide	AT form	ionic strength	K_d (nM)	$10^{-6} \times k_{on}$ ($M^{-1}\,s^{-1}$)	k_{off} (s^{-1})
Idraparinux	α-AT	0.1	0.09 ± 0.04[a]	53 ± 1	0.005 ± 0.002[b]
		0.15	0.44 ± 0.14[a]	32 ± 0.5	0.013 ± 0.003[b]
		0.3	5.0 ± 1.6	16 ± 0.04	0.08 ± 0.03[b]
		0.5	49 ± 3	8.8 ± 0.3	0.4 ± 0.04[b]
		0.6	69 ± 6	5.9 ± 0.06	0.4 ± 0.04[b]
	β-AT	0.1	0.03 ± 0.03[a]	63 ± 2	0.002 ± 0.002[b]
		0.15	0.13 ± 0.096[a]	45 ± 2	0.005 ± 0.004[b]
		0.3	1.5 ± 0.6[a]	21 ± 0.3	0.03 ± 0.01[b]
		0.5	8.3 ± 1.4	8.9 ± 0.5	0.07 ± 0.02[b]
		0.6	20 ± 0.8	5.6 ± 0.3	0.11 ± 0.01[b]
normal	α-AT	0.15	63 ± 10	32 ± 1	1.5 ± 0.4
		0.3	610 ± 40	9.5 ± 0.4	8.9 ± 0.4
		0.5	5800 ± 250[c]	2.5 ± 0.1	14.5 ± 0.3
	β-AT	0.15	18 ± 1	54 ± 1	0.98 ± 0.07[b]
		0.3	190 ± 7	19 ± 0.4	3.6 ± 0.3
		0.5	1030 ± 180[c]	5.9 ± 0.3	6.1 ± 0.7

[a] Obtained by extrapolation of the linear dependence of log K_d on log [Na^+]. [b] Calculated from K_d and k_{on}. [c] Calculated from k_{on} and k_{off}. Dissociation equilibrium constants, K_d, were determined by fluorescence titrations and bimolecular association rate constants, and dissociation rate constants (k_{on} and k_{off}) were determined by stopped-flow fluorimetry as described in Experimental Procedures. The values for K_d are the means ± SE of at least three titrations. k_{on} and k_{off} were determined from the slopes and *y*-intercepts of linear plots of observed pseudo-first-order rate constants, k_{obs}, vs pentasaccharide concentration (inset of Figure 2). k_{on} and k_{off} values ± SE were calculated by linear regression. The data for the normal pentasaccharide, shown for comparison, are taken from ref 18 (*18*).

respectively. About four ionic interactions were involved in the overall binding of the high-affinity pentasaccharide to both α- and β-AT (Table 3), which is similar to what has been shown previously for normal pentasaccharide binding to the two AT forms (*18*). In contrast, the nonionic contribution to the affinity was at least 100-fold higher for the binding of the high-affinity pentasaccharide than for the binding of the normal pentasaccharide to the two forms (Table 3) (*18*). The nonionic dissociation equilibrium constants for high-affinity pentasaccharide binding to α- and β-AT were 450 and 90 nM, respectively (Table 3). The ratio of the free energy of K_d' to that of K_d was calculated ($\Delta G^\circ = -RT \ln K_a$). The nonionic contribution to the free energy was thus found to correspond to ~70% of the total free energy of the overall interaction.

Ionic Contribution to the First Step of Pentasaccharide Binding. The ionic contribution to the initial binding step was resolved in a manner similar to that of the overall binding. Because $k_{on} = k_{+2}/K_1$ and k_{+2} is independent of ionic strength (Table 2), the salt dependence of k_{on} should represent the salt dependence of K_1. Double-logarithmic plots of k_{on} versus [Na^+] were linear for both AT variants (Figure 4), and the number of ionic interactions made in the first binding step could be obtained from the slope of the plots (Table 3). Surprisingly, although about four ionic interactions were involved in the overall binding of both the high-affinity and normal pentasaccharides to α- and β-AT, only ~1 ionic interaction was established in the first step of high-affinity pentasaccharide binding to the two forms, in contrast to the two ionic interactions shown previously for the normal pentasaccharide (*18*). This reduced number of ionic interactions in the first step of high-affinity pentasaccharide binding, therefore, must be compensated for by an increased number of such interactions in the second binding step.

DISCUSSION

This work is an in-depth characterization of the molecular background of the high-affinity binding of a highly negatively charged pentasaccharide, Idraparinux, to α- and β-AT. Idraparinux is a variant of the natural AT-binding pentasaccharide of heparin, in which the four sulfate groups that are essential for the interaction have been essentially maintained. These groups are a 6-O-sulfate group on residue D, a 3-O-sulfate group on residue F, an N-sulfate group on residue F, and an N-sulfate group on residue H. The N-sulfate groups, however, have been replaced by 2-O-sulfate groups (Figure 1) (*31*). Additionally, all OH-groups, one N-sulfate group on residue D, and one O-sulfate group on residue G have been replaced by O-methyl groups. Finally, in comparison with the normal pentasaccharide, one additional 3-O-sulfate group on residue H has been introduced.

Introduction of a 3-O-sulfate group to H-residues of other pentasaccharides has previously been shown to enhance their affinity for AT by increasing the contribution from ionic interactions and hydrogen bonds (*32*). It was, therefore, unexpected that the affinity of Idraparinux, >100-fold higher than that of the normal pentasaccharide for AT, was found to be due mainly to nonionic interactions, whereas the ionic contribution to the overall interaction was the same. The additional nonionic interactions must be established predominantly in the second step of binding of the high-affinity pentasaccharide to AT because the complex formed in the first step is somewhat weaker than that for the normal pentasaccharide. Both rate constants of the second step presumably are affected by these enhanced nonionic interactions. The moderate ~3-fold increase in the forward rate constant is thus most likely a consequence of these interactions because the ionic-strength independence of this rate constant indicates that it is entirely governed by nonionic contacts. Moreover, the ~100-fold decrease in the reverse rate constant of the second step indicates that nonionic interactions also contribute substantially to this decrease. Previous studies have provided strong evidence that the nonreducing end trisaccharide, composed of residues D, E, and F of the normal pentasaccharide, initially recognizes the low-affinity state of AT and subsequently induces and stabilizes

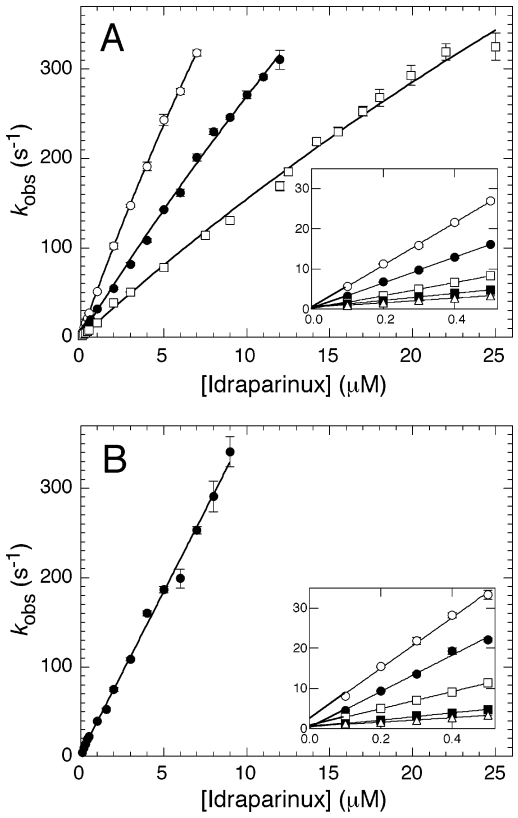

FIGURE 2: Dependence of observed pseudo-first-order rate constants of the interaction between Idraparinux and α- and *β*-AT on Idraparinux concentration in low (inset) and high concentration ranges at 25 °C, pH 7.4, and different ionic strengths. (A) α-AT; (B) *β*-AT. Pseudo-first-order rate constants (k_{obs}) were measured in a stopped-flow instrument as described in Experimental Procedures. The data points represent the mean ± SE of 3−5 k_{obs} values, each derived from three to five fluorescence traces. Data were fit by linear regression to give k_{on} and k_{off} (Table 1) in the low concentration range or by nonlinear regression to give the kinetic constants for the two-step binding mechanism, K_1 and k_{+2} (Table 2) in the high concentration range as described in the Results section. The error bars that are not shown are hidden within the symbols. ○, I 0.1; ●, I 0.15; □, I 0.3 ; ■, I 0.5; △ I 0.6.

Table 2: Kinetic Constants for the Two-Step Mechanism of Idraparinux and Normal Pentasaccharide Binding to α-AT at 25 °C and pH 7.4[a]

pentasaccharide	ionic strength	K_1 (μM)	k_{+2} (s^{-1})	k_{-2} (s^{-1})
Idraparinux	0.1	43 ± 9	2200 ± 400	0.005 ± 0.002
	0.15	84 ± 30	2500 ± 750	0.013 ± 0.003
	0.3	110 ± 40	1900 ± 520	0.08 ± 0.03
normal	0.15	22 ± 2	750 ± 50	1.5 ± 0.6

[a] Dissociation equilibrium constants for the first binding step, K_1, and forward rate constants for the second binding step, k_{+2}, were determined by stopped-flow fluorimetry by fitting the data from the plots in Figure 2 to the rectangular hyperbolic equation (*18*, *24*, *29*). The reverse rate constant for the second binding step, k_{-2}, was taken as k_{off}, calculated from K_d and k_{on} (Table 1). The data for the normal pentasaccharide, shown for comparison, are taken from ref 18 (*18*). Errors represent SE.

the conformational change in the second binding step. In contrast, the two reducing-end residues G and H only serve to stabilize the activated conformation in the second step (*33*, *34*). The enhanced forward rate constant of the second step, which reflects a faster conformational change, presumably is due to an increase in nonionic interactions that involve

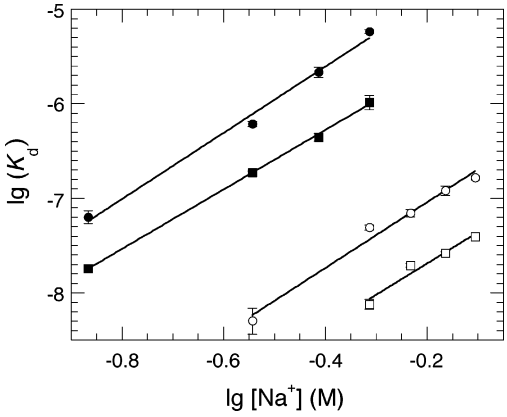

FIGURE 3: Double-logarithmic plots of observed dissociation equilibrium constants vs sodium ion concentration for the interactions between Idraparinux and α- or *β*-AT at 25 °C and pH 7.4. Dissociation equilibrium constants, K_d, were measured by fluorescence titrations at different ionic strengths as described in Experimental Procedures. The data for the normal pentasaccharide, shown for comparison, are taken from ref 18 (*18*). Each data point represents the mean ± SE of 3−5 titrations. Data were fit by linear regression to give the ionic and nonionic contributions to the interaction from the slope and the *y*-intercept, respectively (Table 3), as described in the Results section. The error bars that are not shown are hidden within the symbols. ○, α-AT and Idraparinux; ●, α-AT and normal pentasaccharide; □, *β*-AT and Idraparinux; ■, *β*-AT and normal pentasaccharide.

Table 3: Ionic and Nonionic Contributions to the Interactions of Idraparinux and the Normal Pentasaccharide with α-AT and *β*-AT at 25 °C and pH 7.4[a]

		overall binding		first binding step
pentasaccharide	AT form	Z	K_d' (μM)	Z_1
Idraparinux	α-AT	4.3 ± 0.3	0.45 ± 0.08	1.4 ± 0.06
	β-AT	4.1 ± 0.6	0.09 ± 0.02	1.5 ± 0.1
normal	α-AT	4.4 ± 0.3	62 ± 2	2.4 ± 0.3
	β-AT	3.9 ± 0.1	10 ± 1	2.1 ± 0.2

[a] The number of ionic interactions involved in the overall binding, Z, and in the first binding step, Z_1, was obtained from the slopes of plots of log K_d and log k_{on}, respectively, vs log[Na^+] (Figures 3 and 4). The dissociation equilibrium constant characterizing the nonionic interactions, K_d', was calculated from the *y*-intercept (log K_d') of the log K_d plots. The slopes and intercepts ± SE were obtained by linear regression. The data for the normal pentasaccharide, shown for comparison, are taken from ref 18 (*18*).

the non-reducing end trisaccharide. However, the reduced reverse rate constant of this step, which results in a greater stability of the conformationally activated state, may arise from such tighter interactions involving either or both ends of the pentasaccharide.

The increased nonionic binding contribution is most likely largely due to augmented intermolecular interactions between the high-affinity pentasaccharide and AT, for example, by methyl groups establishing direct hydrophobic contacts with the protein surface. However, the contribution may also be due to an indirect effect. A previous study has thus shown that Phe 122 in the pentasaccharide binding site of AT contributes appreciable free energy of nonionic interactions of high-affinity heparin with AT (*11*), although it does not directly contact the heparin pentasaccharide (*13*). Instead, it is believed to be involved in intramolecular interactions that are necessary for the formation and maintenance of the activated AT conformation (*11*). The binding of the high-

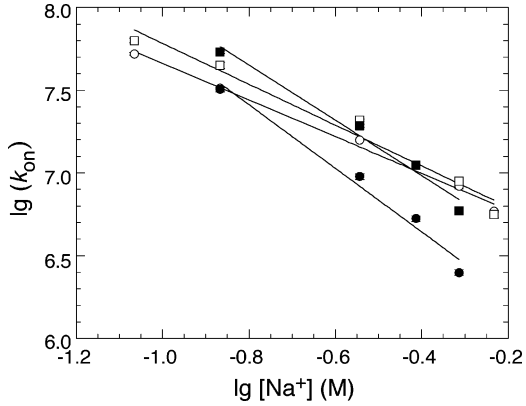

FIGURE 4: Double-logarithmic plots of bimolecular association rate constants vs sodium ion concentration for the interactions between Idraparinux and α- or *β*-AT at 25 °C and pH 7.4. Bimolecular association rate constants, k_{on}, were measured by stopped-flow fluorimetry at different ionic strengths (Figure 2; Table 1) as described in Experimental Procedures. The data for the normal pentasaccharide, shown for comparison, are taken from ref 18 (*18*). Data were fit by linear regression to give the ionic contribution to the first binding step from the slope (Table 3) as described in the Results section. The error bars that are not shown are hidden within the symbols. ○, α-AT and Idraparinux; ●, α-AT and normal pentasaccharide; □, *β*-AT and Idraparinux; ■, *β*-AT and normal pentasaccharide.

affinity pentasaccharide to AT may involve enhanced intramolecular contacts that lead to an increase in the nonionic contribution to the affinity.

Although a total of four ionic interactions are established upon binding of both the high-affinity and normal pentasaccharides to AT, one less ionic interaction is formed in the first step of high-affinity pentasaccharide binding, which most likely is the main reason for the weaker initial complex formation. This loss may reflect the absence of the N-sulfate group present on residue D in the normal pentasaccharide (*33*, *34*). However, this N-sulfate has been reported not to be essential for the interaction with the protein (*31*). Alternatively, a different orientation of the high-affinity pentasaccharide in the binding site during the first step may prevent one of the essential anionic groups of residues D, E, or F from making optimal interactions with AT in the initial complex. The fact that one more ionic interaction is formed in the second step of binding of the high-affinity pentasaccharide than that of the normal pentasaccharide, thereby aiding the nonionic interactions in reducing the reverse rate of the conformational change, presumably is due to the presence of the additional 3-O-sulfate group on residue H. This functional group enhances the affinity of other pentasaccharides for AT (*32*) and is located in the pentasaccharide reducing-end that participates in stabilizing the activated AT conformation in the second step (*13*, *32*, *34*).

The similar fluorescence changes upon interaction of the high-affinity and normal pentasaccharides as well as high-affinity heparin with AT (*24*, *26*, *27*) must reflect identical or highly similar conformational changes that are induced by these saccharides. This conclusion is supported by previous results showing that the three saccharides also enhance the rate of AT inhibition of factor Xa to the same extent (*1*). The higher pharmacological efficiency of the high-affinity pentasaccharide (*21*, *35*), therefore, must primarily reflect the enhanced affinity of this pentasaccharide for AT, which results in a more stable activated complex.

CONCLUSIONS

The highly sulfated, methylated pentasaccharide, Idraparinux, binds tightly to both α- and *β*-AT with an affinity (K_d 0.1−0.4 nM at physiological ionic strength) that is >100-fold higher than that of the normal pentasaccharide. The encounter complex formed in the first binding step is ∼4-fold weaker than that for the latter saccharide, due to only one ionic interaction formed, instead of two. In contrast, the activated AT conformation is ∼400-fold more stable than that induced by the normal pentasaccharide, as a result of both substantially enhanced hydrophobic interactions and one additional ionic interaction. The hydrophobic interactions increase the forward rate constant of the conformational change, whereas both the hydrophobic interactions and the additional ionic interaction aid in locking AT in the activated conformation. The total nonionic contribution to the overall binding is as high as 70%. This study thus shows that nonionic interactions, in addition to ionic interactions, can play a major role in the binding of charged saccharides to proteins and emphasizes the importance of characterizing this nonionic component of binding. Such work will substantially promote the understanding of the nature of glycosaminoglycan−protein interactions and will have major implications for the design of optimal synthetic interaction partners of high medical importance.

ACKNOWLEDGMENT

We thank Professor Ingemar Björk for providing equilibrium binding and kinetic data on normal pentasaccharide binding to antithrombin, valuable discussions, and critical reading of the manuscript.

REFERENCES

1. Olson, S. T., Swanson, R., Raub-Segall, E., Bedsted, T., Sadri, M., Petitou, M., Herault, J. P., Herbert, J. M., and Björk, I. (2004) Accelerating ability of synthetic oligosaccharides on antithrombin inhibition of proteinases of the clotting and fibrinolytic systems. Comparison with heparin and low-molecular-weight heparin, *Thromb. Haemostasis 92*, 929−939.
2. Silverman, G. A., Bird, P. I., Carrell, R. W., Church, F. C., Coughlin, P. B., Gettins, P. G., Irving, J. A., Lomas, D. A., Luke, C. J., Moyer, R. W., Pemberton, P. A., Remold-O'Donnell, E., Salvesen, G. S., Travis, J., and Whisstock, J. C. (2001) The serpins are an expanding superfamily of structurally similar but functionally diverse proteins. Evolution, mechanism of inhibition, novel functions, and a revised nomenclature, *J. Biol. Chem. 276*, 33293−33296.
3. Björk, I., and Olson, S. T. (1997) Antithrombin. A bloody important serpin, *Adv. Exp. Med. Biol. 425*, 17−33.
4. Huntington, J. A. (2006) Shape-shifting serpins−advantages of a mobile mechanism, *Trends Biochem. Sci. 31*, 427−435.
5. Petitou, M., Casu, B., and Lindahl, U. (2003) 1976−1983, a critical period in the history of heparin: the discovery of the antithrombin binding site, *Biochimie 85*, 83−89.
6. Lormeau, J. C., Herault, J. P., Gaich, C., Barzu, T., van Dinther, T. G., Visser, A., and Herbert, J. M. (1997) Determination of the anti-factor Xa activity of the synthetic pentasaccharide SR 90107A/ORG 31540 and of two structural analogues, *Thromb. Res. 85*, 67−75.
7. Arocas, V., Bock, S. C., Olson, S. T., and Björk, I. (1999) The role of Arg46 and Arg47 of antithrombin in heparin binding, *Biochemistry 38*, 10196−10204.
8. Desai, U., Swanson, R., Bock, S. C., Björk, I., and Olson, S. T. (2000) Role of arginine 129 in heparin binding and activation of antithrombin, *J. Biol. Chem. 275*, 18976−18984.
9. Arocas, V., Bock, S. C., Raja, S., Olson, S. T., and Björk, I. (2001) Lysine 114 of antithrombin is of crucial importance for the affinity

and kinetics of heparin pentasaccharide binding, *J. Biol. Chem. 276*, 43809−43817.
10. Schedin-Weiss, S., Desai, U. R., Bock, S. C., Gettins, P. G., Olson, S. T., and Björk, I. (2002) Importance of lysine 125 for heparin binding and activation of antithrombin, *Biochemistry 41*, 4779−4788.
11. Jairajpuri, M. A., Lu, A., Desai, U., Olson, S. T., Björk, I., and Bock, S. C. (2003) Antithrombin III phenylalanines 122 and 121 contribute to its high affinity for heparin and its conformational activation, *J. Biol. Chem. 278*, 15941−15950.
12. Schedin-Weiss, S., Desai, U. R., Bock, S. C., Olson, S. T., and Björk, I. (2004) Roles of N-terminal region residues Lys11, Arg13, and Arg24 of antithrombin in heparin recognition and in promotion and stabilization of the heparin-induced conformational change, *Biochemistry 43*, 675−683.
13. Jin, L., Abrahams, J. P., Skinner, R., Petitou, M., Pike, R. N., and Carrell, R. W. (1997) The anticoagulant activation of antithrombin by heparin, *Proc. Natl. Acad. Sci. U.S.A. 94*, 14683−14688.
14. Li, W., Johnson, D. J., Esmon, C. T., and Huntington, J. A. (2004) Structure of the antithrombin-thrombin-heparin ternary complex reveals the antithrombotic mechanism of heparin, *Nat. Struct. Mol. Biol. 11*, 857−862.
15. Dementiev, A., Petitou, M., Herbert, J. M., and Gettins, P. G. (2004) The ternary complex of antithrombin-anhydrothrombin-heparin reveals the basis of inhibitor specificity, *Nat. Struct. Mol. Biol. 11*, 863−867.
16. Johnson, D. J., Li, W., Adams, T. E., and Huntington, J. A. (2006) Antithrombin-S195A factor Xa-heparin structure reveals the allosteric mechanism of antithrombin activation, *EMBO J. 25*, 2029−2037.
17. Schedin-Weiss, S., Arocas, V., Bock, S. C., Olson, S. T., and Björk, I. (2002) Specificity of the basic side chains of Lys114, Lys125, and Arg129 of antithrombin in heparin binding, *Biochemistry 41*, 12369−12376.
18. Turk, B., Brieditis, I., Bock, S. C., Olson, S. T., and Björk, I. (1997) The oligosaccharide side chain on Asn-135 of alpha-antithrombin, absent in beta-antithrombin, decreases the heparin affinity of the inhibitor by affecting the heparin-induced conformational change, *Biochemistry 36*, 6682−6691.
19. Choay, J., Petitou, M., Lormeau, J. C., Sinay, P., Casu, B., and Gatti, G. (1983) Structure-activity relationship in heparin: a synthetic pentasaccharide with high affinity for antithrombin III and eliciting high anti-factor Xa activity, *Biochem. Biophys. Res. Commun. 116*, 492−499.
20. de Kort, M., Buijsman, R. C., and van Boeckel, C. A. (2005) Synthetic heparin derivatives as new anticoagulant drugs, *Drug. Discovery Today 10*, 769−779.
21. Herbert, J. M., Herault, J. P., Bernat, A., van Amsterdam, R. G., Lormeau, J. C., Petitou, M., van Boeckel, C., Hoffmann, P., and Meuleman, D. G. (1998) Biochemical and pharmacological properties of SANORG 34006, a potent and long-acting synthetic pentasaccharide, *Blood 91*, 4197−4205.
22. Olson, S. T., Björk, I., and Shore, J. D. (1993) Kinetic characterization of heparin-catalyzed and uncatalyzed inhibition of blood coagulation proteinases by antithrombin, *Methods Enzymol. 222*, 525−559.
23. Nordenman, B., Nystrom, C., and Björk, I. (1977) The size and shape of human and bovine antithrombin III, *Eur. J. Biochem. 78*, 195−203.
24. Olson, S. T., Björk, I., Sheffer, R., Craig, P. A., Shore, J. D., and Choay, J. (1992) Role of the antithrombin-binding pentasaccharide in heparin acceleration of antithrombin-proteinase reactions. Resolution of the antithrombin conformational change contribution to heparin rate enhancement, *J. Biol. Chem. 267*, 12528−12538.
25. Long, G. L., Kjellberg, M., Villoutreix, B. O., and Stenflo, J. (2003) Probing plasma clearance of the thrombin-antithrombin complex with a monoclonal antibody against the putative serpin-enzyme complex receptor-binding site, *Eur. J. Biochem. 270*, 4059−4069.
26. Nordenman, B., Danielsson, Å., and Björk, I. (1978) The binding of low-affinity and high-affinity heparin to antithrombin. Fluorescence studies, *Eur. J. Biochem. 90*, 1−6.
27. Olson, S. T., and Shore, J. D. (1981) Binding of high affinity heparin to antithrombin III. Characterization of the protein fluorescence enhancement, *J. Biol. Chem. 256*, 11065−11072.
28. Olson, S. T., and Björk, I. (1991) Predominant contribution of surface approximation to the mechanism of heparin acceleration of the antithrombin-thrombin reaction. Elucidation from salt concentration effects, *J. Biol. Chem. 266*, 6353−6364.
29. Olson, S. T., Srinivasan, K. R., Björk, I., and Shore, J. D. (1981) Binding of high affinity heparin to antithrombin III. Stopped flow kinetic studies of the binding interaction, *J. Biol. Chem. 256*, 11073−11079.
30. Record, M. T., Jr., Lohman, M. L., and De Haseth, P. (1976) Ion effects on ligand-nucleic acid interactions, *J. Mol. Biol. 107*, 145−158.
31. Petitou, M., and van Boeckel, C. A. (2004) A synthetic antithrombin III binding pentasaccharide is now a drug! What comes next? *Angew. Chem., Int. Ed. 43*, 3118−3133.
32. Desai, U. R., Petitou, M., Björk, I., and Olson, S. T. (1998) Mechanism of heparin activation of antithrombin: evidence for an induced-fit model of allosteric activation involving two interaction subsites, *Biochemistry 37*, 13033−13041.
33. Petitou, M., Barzu, T., Herault, J. P., and Herbert, J. M. (1997) A unique trisaccharide sequence in heparin mediates the early step of antithrombin III activation, *Glycobiology 7*, 323−327.
34. Desai, U. R., Petitou, M., Björk, I., and Olson, S. T. (1998) Mechanism of heparin activation of antithrombin. Role of individual residues of the pentasaccharide activating sequence in the recognition of native and activated states of antithrombin, *J. Biol. Chem. 273*, 7478−7487.
35. van Boeckel, C. A. A., and Petitou, M. (1993) The unique antithrombin III binding domain of heparin: a lead to new synthetic antithrombotics, *Angew. Chem., Int. Ed. Engl. 32*, 1671−1818.

BI6024929